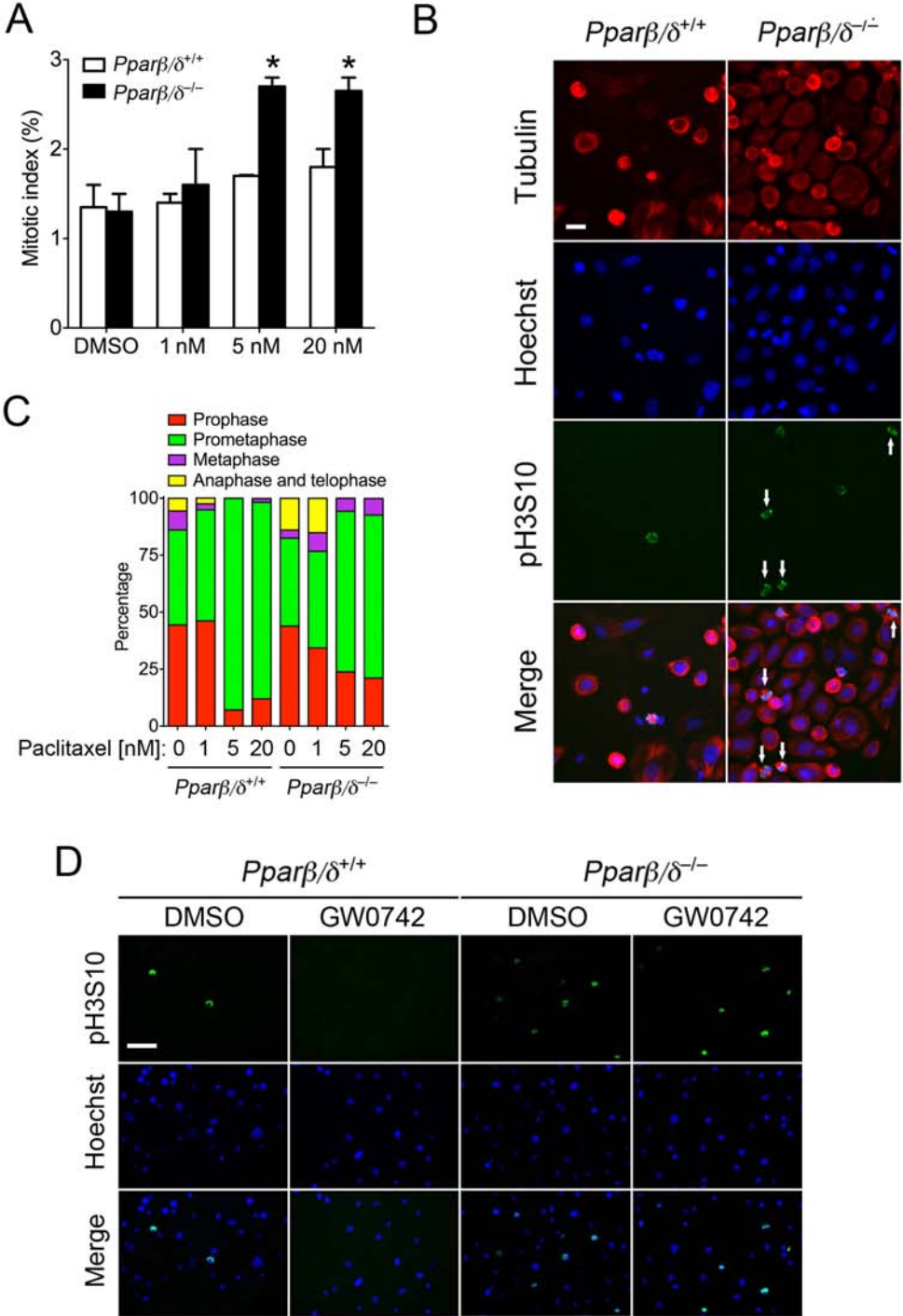
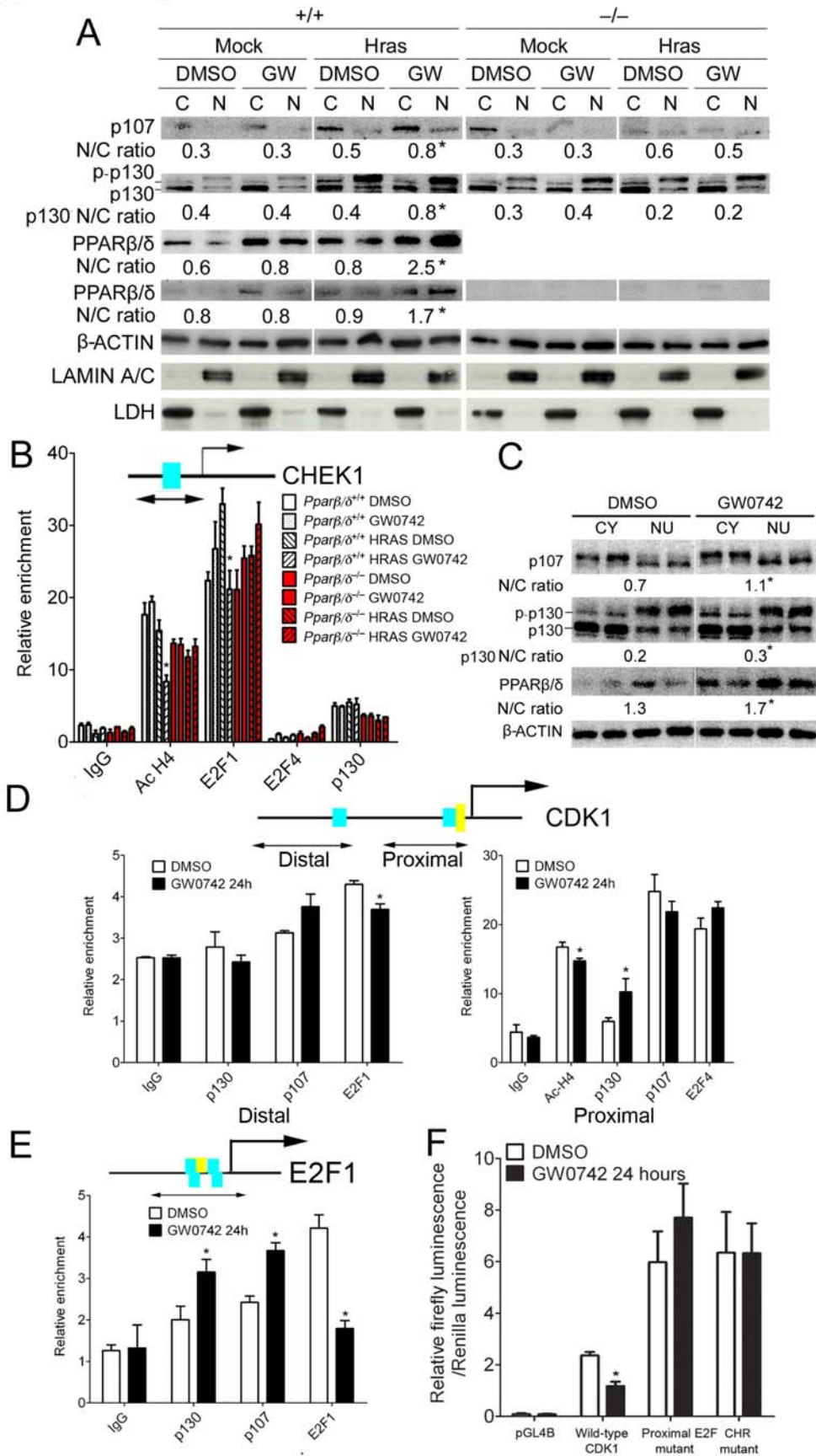


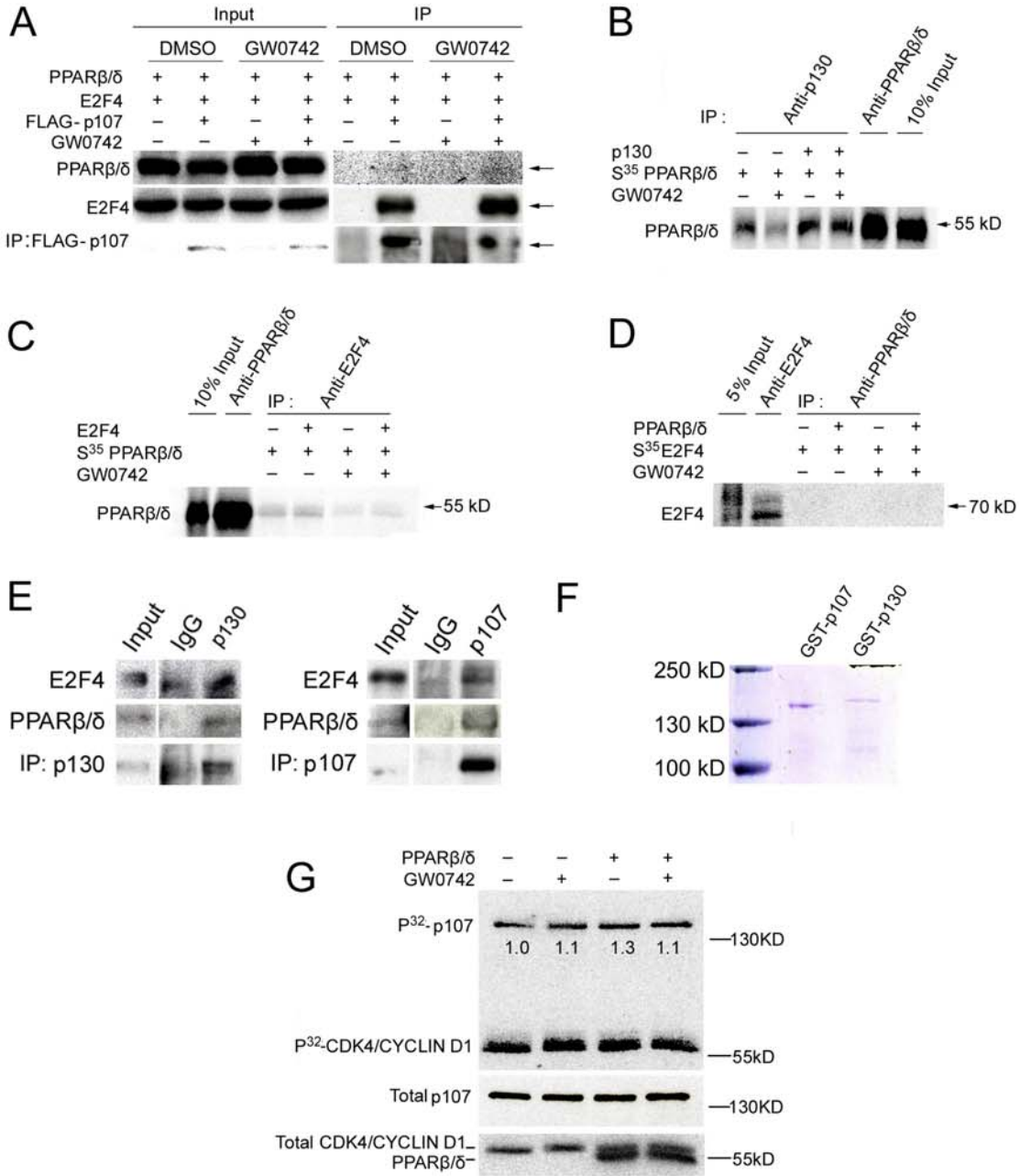
Supplemental Fig. 2, Zhu et al



Supplemental Fig. 3, Zhu et al



Supplemental Fig. 4, Zhu et al



1 **Supplemental Figure legends**

2

3 FIG. S1. Ligand activation of PPAR $\beta/\delta$  inhibits HRAS-expressing keratinocyte  
4 proliferation by inducing G2/M arrest and selects against highly expressing HRAS-  
5 expressing keratinocytes. HRAS-expressing wild-type and *Ppar $\beta/\delta$* -null keratinocytes  
6 were treated with or without 1  $\mu$ M GW0742 for 3 d (A) Cell cycle analysis was  
7 performed with bromodeoxyuridine/propidium iodide (PI) labeling followed by flow  
8 cytometry. (B) Representative DNA histograms from flow cytometric analysis of PI in  
9 HRAS-expressing keratinocytes treated with or without 1  $\mu$ M GW0742 for 9 d. (C)  
10 Quantified distribution of cells in the different phases of the cell cycle from samples in  
11 (B). (D) Western blot analysis of CDK4, CYCLIN D1, and CYCLIN B1 from HRAS-  
12 expressing keratinocytes treated with or without 1  $\mu$ M GW0742 for 9 d. Hybridization  
13 signals for each protein was normalized to that of ACTIN and are presented as fold  
14 change relative to control DMSO. (E) HRAS-expressing wild-type and *Ppar $\beta/\delta$* -null  
15 keratinocytes were treated with or without 1  $\mu$ M GW0742 for 3 d and qPCR was  
16 performed to quantify copy number of genomic *Hras* DNA. (F) Mock-infected or HRAS-  
17 expressing keratinocytes with increasing M.O.I. were treated with or without 1  $\mu$ M  
18 GW0742 for 24 or 72 h and *Hras* mRNA expression was measured by qPCR. (G)  
19 HRAS-expressing keratinocytes with increasing M.O.I. were treated with or without 1  
20  $\mu$ M GW0742 for 3 d and the percentage of cells in different phases of the cell cycle was  
21 determined by flow cytometry after PI staining. (H) HRAS-expressing keratinocytes  
22 were treated with or without 1  $\mu$ M GW0742, 5 nM paclitaxel or 10 nM paclitaxel for 3 d.  
23 Representative flow cytometric analysis after labeling with an anti-HRAS antibody is

24 shown for each treatment. For all datasets, N = 3-4 independent samples per treatment  
25 group. Values represent the mean  $\pm$  SEM. \*significantly different than wild-type vehicle  
26 control (DMSO) group,  $P \leq 0.05$ . #significantly less than wild-type control,  $P \leq 0.05$ .  
27 Values with different letters are significantly different,  $P \leq 0.05$ .

28  
29 FIG. S2. PPAR $\beta/\delta$  delays entry into mitosis of HRAS-expressing keratinocytes. (A-C)  
30 HRAS-expressing wild-type and *Ppar $\beta/\delta$* -null keratinocytes were cultured for 4 d and  
31 then treated with paclitaxel for 24 h. (A) Cells were immunostained to determine the  
32 mitotic index. (B) Representative photomicrographs of immunostained keratinocytes.  
33 Arrowheads indicate cells with a metaphase plate on a bipolar spindle. A significant  
34 number of HRAS-expressing *Ppar $\beta/\delta$* -null keratinocytes showed fully aligned  
35 chromosomes at metaphase plate after 20 nM paclitaxel treatment. Scale bar = 10  $\mu$ m.  
36 (C) The distribution of cells in different mitotic phases was determined as described in  
37 Materials and methods. (D) Representative photomicrographs of HRAS-expressing  
38 keratinocytes synchronized at the G2 phase by treatment with 15  $\mu$ M RO-3306 (CDK1  
39 inhibitor) and then released into nocodazole (to block the cells at prometaphase) with or  
40 without 1  $\mu$ M GW0742 for 12 hours. Note the decrease in the number of pH3S10-  
41 positive cells in GW0742-treated wild-type keratinocytes. Scale bar = 50  $\mu$ m. For all  
42 datasets, N  $\geq$  3 independent samples per treatment group. Values represent the mean  $\pm$   
43 SEM. \*significantly greater than control,  $P \leq 0.05$ .

44  
45 FIG. S3. Effect of ligand activation of PPAR $\beta/\delta$  on nuclear accumulation and promoter  
46 occupancy of p130/p107 and/or E2F in keratinocytes and 308 cells. Wild-type and

47 *Pparβ/δ*-null keratinocytes were mock infected or infected with an *Hras* encoding  
48 retrovirus for 2 d. Cells were cultured with or without 1 μM GW0742 for 24 h. (A)  
49 Western blot analysis of p130, p107, E2F4 and PPARβ/δ in cytosol (C) and nuclear (N)  
50 extracts. Expression levels were normalized to β-ACTIN. The average ratio of nuclear to  
51 cytoplasmic protein (N/C) is shown. Promoter occupancy of acetylated histone 4 (AC-  
52 H4), E2F1, E2F4 and p130 was examined by ChIP analysis of the mouse (B) CHEK1  
53 promoter. For the CHEK1 promoter, the E2F1 activator binding site is depicted as a  
54 blue box. The relative position of the PCR products used for ChIP analysis is shown by  
55 the lines with double arrows. (C) 308 cells were cultured to near confluency and then  
56 treated with DMSO or 1 μM GW0742 for 24 hours. Western blot analysis of p107, p130  
57 and PPARβ/δ in cytosol (C) and nuclear (N) extracts. The average ratio of nuclear to  
58 cytoplasmic protein (N/C) is shown. Promoter occupancy of AC-H4, E2F1, p130, p107  
59 and E2F4 was examined by ChIP analysis of the mouse (D) CDK1 or (E) E2F1  
60 promoter in 308 cells. For the CDK1 and E2F1 promoter, the distal E2F1 activator  
61 binding site and the proximal E2F4 repressor binding site is depicted as two blue boxes  
62 and the CHR binding site is depicted as the yellow box. The relative position of the PCR  
63 products used for ChIP analysis is shown by the lines with double arrows. (F) Promoter  
64 analysis of the mouse CDK1 promoter. Mutations in the proximal repressor E2F4  
65 binding site and the proximal CHR are described in the Materials and methods. For all  
66 datasets, N = 3 independent samples. Values represent the mean ± S.E.M..  
67 \*significantly different than DMSO control,  $P \leq 0.05$ .

68

69 FIG. S4. PPAR $\beta/\delta$  binds with p107/p130. (A) Co-immunoprecipitations using HEK293T  
70 cells transiently transfected with FLAG-p107, pCMV-E2F4 and pSG5-PPAR $\beta/\delta$ , treated  
71 with DMSO or 1 $\mu$ M GW0742 for 24 hours. (B) Co-immunoprecipitations of *in vitro*  
72 translated p130 and <sup>35</sup>S-labeled PPAR $\beta/\delta$  in the absence or presence of 1 $\mu$ M GW0742.  
73 (C, D) Co-immunoprecipitations of *in vitro* translated E2F4 and <sup>35</sup>S-labeled PPAR $\beta/\delta$  (C)  
74 or <sup>35</sup>S-labeled E2F4 and PPAR $\beta/\delta$  (D) in the absence or presence of 1  $\mu$ M GW0742. (E)  
75 Interaction between endogenous p130/p107 and PPAR $\beta/\delta$  in HEK293T cells. (F)  
76 Commassie staining of affinity purified recombinant GST-p107 and GST-p130 protein  
77 isolated from *E. coli*. (G) *In vitro* kinase assay with recombinant GST-p107. GST-p107  
78 was pre-incubated with dilution buffer or recombinant human PPAR $\beta/\delta$  in the presence  
79 of DMSO or 1  $\mu$ M GW0742 before <sup>32</sup> $\gamma$ -ATP and a CDK4/CYCLIN D1 complex were  
80 added. The reaction was stopped by adding SDS loading buffer and resolved by SDS-  
81 PAGE and the amount of phosphorylated p107 was determined by autoradiography.  
82 The ratio of the phosphorylated p107 relative to total p107 is shown below each band.